INVESTIGATION OF BAFFLE EFFECT ON FLUID FLOW AND HEAT TRANSFER INTO TRAPEZOIDAL CAVITIES

Éliton Fontana, eliton_fontana@hotmail.com
Adriano da Silva, adriano@unochapeco.edu.br
Universidade Comunitária Regional de Chapecó – UNOCHAPECÓ
Rua Senador Atílio Fontana, 591 E, CEP: 89809-000, Chapecó, SC, Brasil

Andre de Souza Araújo, andre@cefet-ce.br
Instituto Federal de Educação, Ciência e Tecnologia do Ceará

Francisco Marcondes, marcondes@ufc.br
Departamento de Engenharia Metalúrgica e de Materiais – UFC
Caixa Postal 12144, Fortaleza, CE, Brasil

Viviana Cocco Mariani, viviana.mariani@pucpr.br
Programa de Pós-Graduação em Engenharia Mecânica – PUCPR
Rua Imaculada Conceição, 1155, Prado Velho, CEP: 81611-970, Curitiba, PR, Brasil

Abstract. *The fluid flow and heat transfer in a trapezoidal cavity were numerically analyzed in this paper. The bottom horizontal and upper inclined walls are adiabatic, while the vertical walls are isothermal. For the later mentioned walls, two thermal boundary conditions are considered. In the first one, the left short vertical wall is heated while the right long vertical wall is cooled. In the second one, the right long vertical wall is heated while the left short vertical wall is cooled. The governing equations are solved through the finite-volume method, considering steady state, two-dimensional system and laminar conditions. Computations were carried out to examine the effects of the number of baffles (1 or 2), length (W_b=L/20) and location (L_b=L/3 or 2L/3, L_{b1} = L/3 and L_{b2} = 2L/3), and Rayleigh number ($10^3 \leq Ra \leq 10^6$). Results are displayed in terms of streamlines, isotherms, and local and average Nusselt numbers. The results from several case studies are presented to investigate the effect of the investigated parameters.*

Keywords*: natural convection, trapezoidal cavities, finite-volume method, internal baffles.*

1. INTRODUCTION

In recent years, the natural convection in cavities has been extensively investigated due to the practical interest in many fields of science and technology. Its application includes food processing and storage, thermal insulation of buildings, electrochemistry, fire control, metallurgy, meteorology, geophysics, among them.. One of the basic problems concerning the natural convection in rectangular cavities is the one whose vertical walls are maintained at different constant temperatures and the top and bottom walls are adiabatic. Gebhart (1979) and Hoogendoorn (1986) emphasized various aspects of natural convection flows in a square cavity. Ostrach (1988) and Bejan (2004) explained that the internal natural convection flow problems are more complex than the external ones, due to the interaction between the boundary layer and core and because the core flow is very sensitive to the geometry and to the boundary conditions. Several attempts have been made to shed some light on the natural convection flows into enclosures. Among of them, we can cite the works of Patterson and Imberger (1980), Nicolette et al. (1985), Hall et al. (1988), Hyun and Lee (1989), Fusegi et al. (1992), Lage and Bejan (1991), and Xia and Murthy (2002).

However, most of these studies are restricted to the cases of simple geometry like rectangular, square, cylindrical and spherical cavities. Among the earlier reported studies for triangular enclosures, Karyakin et al. (1988) and Holtzman et al. (2000) described laminar natural convection in isosceles triangular enclosures heated from below and symmetrically cooled from above. Buoyancy driven flows are complex because of essential coupling between the transport properties of the flow and thermal fields. Del Campo et al. (1988) modeled the steady state natural convection in triangular enclosures in conjunction with a stream function–vorticity formulation for two aspect ratio and Grashof equal to 10^3 and 10^6. Their investigation is based on a symmetric boundary condition for a system heated from below. The solutions obtained were symmetric about the middle plane. Poulikakos and Bejan (1983) investigated the fluid dynamics inside a triangular enclosure. They applied the asymptotic methods of Cormack et al. (1974) to find approximate steady state regime and temperature distributions inside cavity when aspect ratio of the enclosure is vanishing. This led to the criteria, in the steady state, for the existence of distinct thermal and viscous layers along both the walls. This physical complexity in confined cavities is not only a topic for analysis but also has equal significance for numerical and experimental investigations.

Few researches have paid attention to the natural convection in trapezoidal cavities. Iyican et al. (1980a, 1980b) investigated experimentally and numerically the flow and heat transfer into the trapezoidal enclosure with parallel top and bottom walls at different temperatures and adiabatic plane walls. A critical Rayleigh number was presented

depending on the angle. Lam et al. (1989) reported similar results for a trapezoidal cavity composed of two vertical adiabatic side walls, a horizontal hot bottom wall, and an inclined cold top wall. Karyakin (1989) has shown the transient results for the natural convection in an isosceles trapezoidal cavity inclined at angle ϕ to the vertical wall, where a single circulation region is found when the steady state case is investigated. The heat transfer rate is found to increase with the increase in the angle ϕ.

Lee (1984, 1991) presented numerical results, to Rayleigh numbers up to 10^5, for natural convection in trapezoidal enclosures. Peric (1993) studied natural convection in the same geometry with refined grids and observed the convergence of results for independent grids. Computations in the same geometry were carried out by Sadat and Salagnac (1995) with Rayleigh number ranging from 10^3 to 2×10^5. Kuyper and Hoogendoorn (1995) using the same geometry investigated the influence of the inclination angle on the flow and also the dependence of the average Nusselt number on the Rayleigh number on laminar natural convection flow in trapezoidal enclosures. Moukalled and Acharya (1997, 2000, 2001) dealt with natural-convection heat transfer in a partially divided trapezoidal cavity with partial dividers attached to the lower horizontal base or the upper inclined surface of the cavity. In that last work, however, two offset baffles were employed. Heat transfer within trapezoidal cavity heated at the bottom and cooled at the inclined top part was investigated by Boussaid et al. (2003). Natural convection in another partitioned trapezoidal cavity heated from the side has been studied numerically by Moukalled and Darwish (2003). The effects of Rayleigh and Prandtl numbers, baffle height and location on heat transfer were investigated for two boundary conditions in that work. The baffles decrease heat transfer, with its rate increasing with the increasing Prandtl number and height baffle.

In the present study the cavity has upper inclined and lower horizontal walls are insulated, and the left and right vertical walls were either heated or cooled (uniformly) by means of a constant temperature, respectively. So, the boundary conditions are equal to Moukalled and Darwish (2003), however in the present work, the effect of one or two baffles inside of trapezoidal cavity are investigated. Similar to the works of Moukalled and Acharya (1997), and Moukalled and Darwish (2003) the baffles are attached to the lower horizontal base of the cavity. The finite-volume method has been used to solve the nonlinear coupled partial differential equations for flow and temperature fields. The main goal of the present paper is to study the circulations and temperature distributions within the trapezoidal cavity and the heat transfer rate at the walls in terms of local and average Nusselt numbers.

2. PHYSICAL MODEL AND GOVERNING EQUATIONS

The general schematic configurations of the two-dimensional trapezoidal cavities (with one and two inside baffles) are shown in Fig. 1(a) along with the coordinates and boundary conditions. The grid distributions for numerical solution are shown in Fig. 1(b). The vertical walls of the trapezoidal cavity are heated and/or cooled at constant temperatures T_H and T_C, respectively, where $T_H > T_C$. The horizontal and inclined walls are kept adiabatic. The width of the cavity (L) is 4 times the height (H) of the shortest vertical wall. The inclination of the upper wall of the cavity is fixed at 15°. One baffle height ($H_b = H_{b1} = H_{b2} = 2H^*/3$), where H^* is the height of the cavity at the location of baffle, one baffle thickness ($W_b = L/20$), and two baffle locations ($L_b = L/3$ or $L_b = 2L/3$, $L_{b1} = L/3$ and $L_{b2} = 2L/3$) are considered.

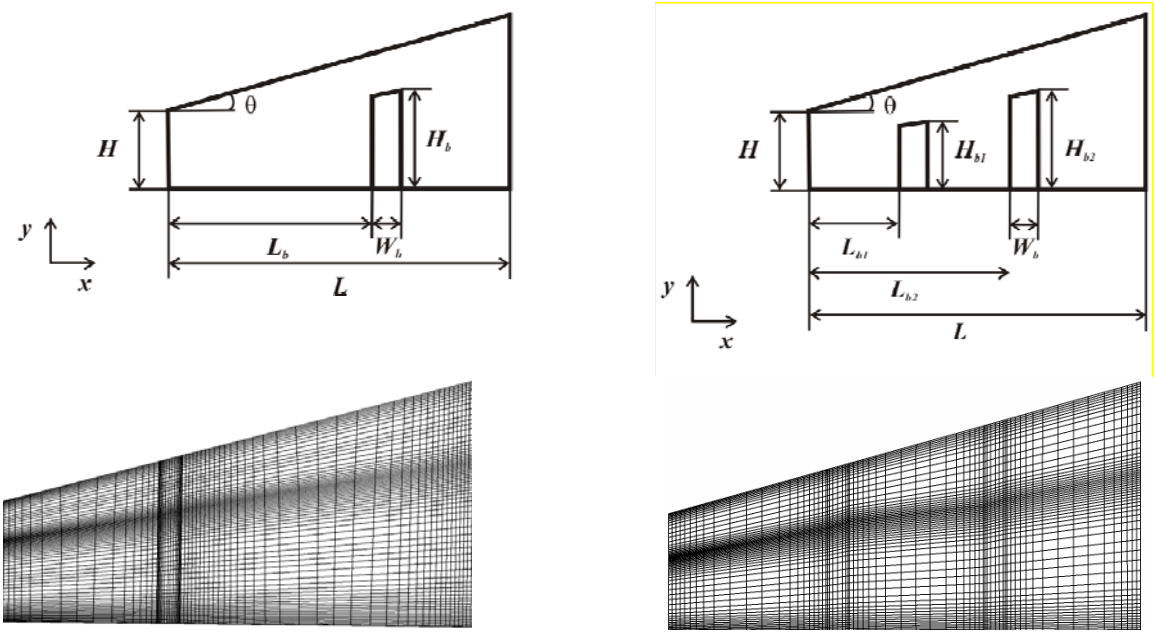

Figure 1. (a) Physical model. (b) Grid distribution.

The fluid properties are assumed constant except for the variation of density in the buoyancy force term of the momentum equation in the *y* direction which is approximated by the Boussinesq approximation. Meanwhile, the flow field is considered to be steady state, laminar, and two-dimensional. Thus the governing equations for the fluid flow and heat transfer are those expressing the conservation of mass, momentum, and energy. In dimensional form, the transport equations are given by

$$\frac{\partial u}{\partial x}+\frac{\partial v}{\partial y}=0\,, \tag{1}$$

$$\frac{\partial (uu)}{\partial x}+\frac{\partial (vu)}{\partial y}=-\frac{1}{\rho}\frac{\partial p}{\partial x}+\frac{\partial}{\partial x}\left(\nu\frac{\partial u}{\partial x}\right)+\frac{\partial}{\partial y}\left(\nu\frac{\partial u}{\partial y}\right), \tag{2}$$

$$\frac{\partial (uv)}{\partial x}+\frac{\partial (vv)}{\partial y}=-\frac{\partial p}{\partial y}+\frac{\partial}{\partial x}\left(\nu\frac{\partial v}{\partial x}\right)+\frac{\partial}{\partial y}\left(\nu\frac{\partial v}{\partial y}\right)+\rho\beta(T_0-T)g\,, \tag{3}$$

$$\frac{\partial (uT)}{\partial x}+\frac{\partial (vT)}{\partial y}=\frac{\partial}{\partial x}\left(\alpha\frac{\partial T}{\partial x}\right)+\frac{\partial}{\partial y}\left(\alpha\frac{\partial T}{\partial y}\right), \tag{4}$$

where u (m/s) is the velocity in x-direction; v (m/s) the velocity in the y-direction, ρ (kg/m^3) is the fluid density, μ (Pa.s) is dynamic viscosity, ν (m^2/s) is kinematic viscosity, α (m^2/s) is the thermal diffusivity ($\alpha = k/\rho c_p$), β (1/K) is the thermal expansion coefficient of air, T_0 (K) is the reference temperature, T (K) is the temperature, and g (m/s^2) is the gravity acceleration.

The boundary conditions associated with the governing equations (Eqs. (1) to (4)) used in this investigation are given below. The definition of x and y co-ordinates can be seen in Fig. 1(a). Two thermal boundary conditions are considered. Thus, temperature boundary conditions on the vertical surfaces in the first case are

$$T(x = 0, y) = T_{C,} \tag{5}$$
$$T(x = L, y) = T_H. \tag{6}$$

In the second case these temperatures are change by $T(x = 0, y) = T_H$ and $T(x = L, y) = T_{C.}$ No-slip velocities on surfaces were assumed as shown in Eqs. (7) through (10),

$$u(x=0,y)=v(x=0,y)=0\,, \tag{7}$$
$$u(x=L,y)=v(x=L,y)=0\,, \tag{8}$$
$$u(x,y=0)=v(x,y=0)=0\,, \tag{9}$$
$$u(x,y=H+xtg(\theta))=v(x,y=H+xtg(\theta))=0\,. \tag{10}$$

The bottom and top walls were kept insulated.

$$\left.\frac{\partial T}{\partial y}\right)_{y=0}=0\,, \tag{11}$$

$$\left.\frac{\partial T}{\partial y}\right)_{y=H+xtg(\theta)}=0 \tag{12}$$

The energy balance at the baffle-air interface can be stated as

$$-\frac{1}{Pr}(\hat{n}.\vec{\nabla}\theta)_i=-\frac{k_r}{Pr}(n.\vec{\nabla}\theta_b)_i\,, \tag{13}$$

where $\hat{n}$ is a unit vector normal to the baffle-air interface, the subscript i refers to the interface, and k_r is the ratio between the thermal conductivity of the baffle and the convective fluid. The Rayleigh number is defined by $Ra = g\beta(T_H - T_C)H^3/\nu\alpha$.

3. NUMERICAL METHODOLOGY AND ANALYSIS

The numerical solution of the governing equations was performed using the commercial computational fluid dynamics code Ansys CFX version 11.0. In this code, the conservation equations for mass, momentum and turbulence quantities are solved using the finite-volume method generated by structured grids. For this practice the solution domain is divided into small control volumes and the governing differential equations are integrated over each control volume with use of the Gauss theorem. The resulting discrete system of linear equations is solved using an algebraic multigrid methodology called additive correction accelerated incomplete lower upper (ILU) factorization technique. It is an iterative solver whereby the exact solution of the equations is approached during the course of several iterations. The solution was considered converged when the sum of absolute normalized residuals for all cells in the flow domain became less than 10^{-5}.

3.1. Comparing Grids

The local and average Nusselt numbers along the hot or cold wall were computed from

$$Nu = \frac{hl}{k} \tag{14}$$

$$\overline{Nu} = \frac{1}{l}\int_0^l Nu dx \tag{15}$$

where l is the height of the hot or cold wall, and h (W/m^{2}K) is the heat transfer coefficient. Based on this definition, the average Nusselt numbers along both walls are equal. In the present section, the number of volumes required to obtain a grid independent solution is determined by the local Nusselt numbers with distribution along the cold and hot walls for Ra = 10^4 and 10^5. Note that grid-independence tests have been conducted for all the configurations studied in this work. The refinement was mainly promoted at the walls of the cavity and next to baffle(s), where is expected the gradients to be higher. Three different computational non-uniform grids composed by 30×32, 60×64, and 120×128 grids were used, and some results obtained are presented in Figs. 2 and 3.

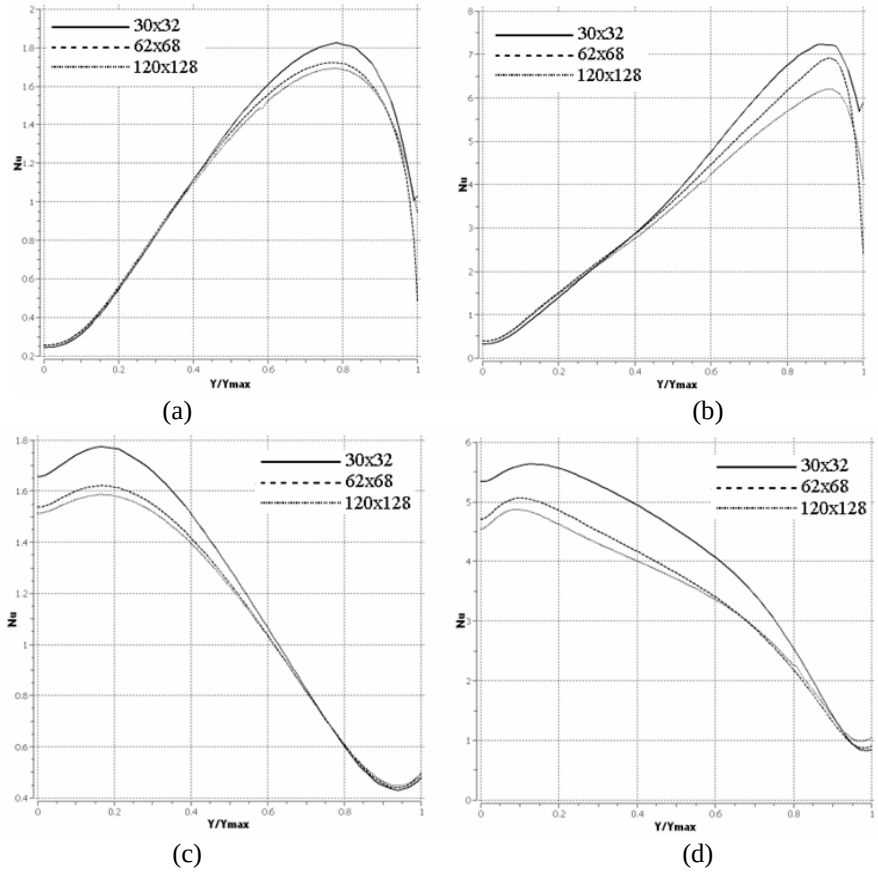

Figure 2. Computational grids influence on local Nusselt numbers: Distribution along the (a, b) cold and (c, d) hot walls, for (a, c) Ra = 10^4 and (b, d) Ra = 10^5, for the buoyancy-assisting boundary condition (left wall hot), $H_b = 2H^*/3$, $L_b = L/3$.

The numerical validation was conducted in terms of the local Nusselt numbers in two different positions along the cold and hot walls, as detailed in Figs. 2 and 3, for the buoyancy-assisting boundary condition (left hot wall) and buoyancy opposing boundary condition (right hot wall), respectively. The computational grid independently solution for the domain with the left wall hot can be seen in Fig. 2(a, c) for Ra = 10^4 and Fig. 2(b, d) for Ra = 10^5, and with the right hot wall can be seen in Fig. 3(a, c) for Ra = 10^4 and Fig. 3(b, d) for Ra = 10^5. Because of the minor differences between the 60×64 and 120×128 grids, the 60×64 non-uniform grid was chosen for all the simulations presented in this work.

The Nusselt distributions along the cold and hot walls obtained in a partitioned enclosure of baffle height H_b = 2H*/3 located at L_b = L/3 are compared in Figs. 3(a, b) and 3(c, d), respectively. As shown, the Nusselt levels increase with increasing Rayleigh numbers.

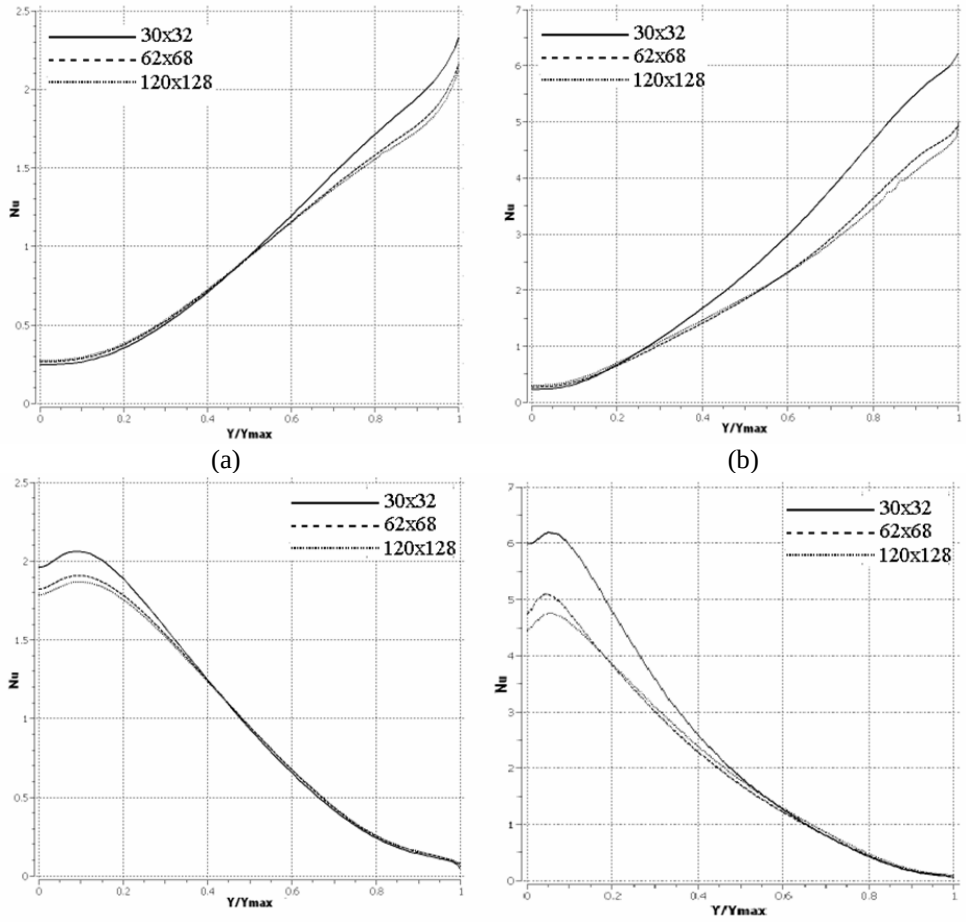

Figure 3. Computational grids influence on local Nusselt numbers: Distribution along the (a, b) cold and (c, d) hot walls, for (a, c) Ra = 10^4 and (b, d) Ra = 10^5, for the buoyancy-opposing boundary condition (right wall hot)), H_b = 2H*/3, L_b = L/3.

3.2. Numerical Validation for one baffle

In order to compare the numerical solution of the present study, some solutions obtained in trapezoidal cavity with one baffle inside have been compared with some of results obtained by Moukalled and Darwish (2003). Figs. 4 and 5 present the isotherms and streamlines, respectively and Tabs. 1 through 4, the average Nusselt number for for L_b = L/3 and H_b = 2H*/3 and Pr=0,7.

Isotherms presented in Figure 4 reflect that at low Rayleigh, variations in temperature are almost uniform over the domain, indicating dominant conduction heat transfer mode. As Rayleigh increases, convection is promoted, and isotherms become more distorted. Streamlines in Fig. 5 indicates that at the lowest Rayleigh presented, Ra = 10^3, the recirculation flow exhibits two vortices communicating through a very thin overall rotating eddy (Fig. 5a). These two vortices rotate in the clockwise direction. As Ra increases, communication between the vortices increases until at Ra = 10^5 the two vortices merge into one, see Fig. 5c. Moreover, with increasing values of Rayleigh, the flow between the baffle and the cold wall becomes weaker as compared to the region between the baffle and the hot wall. The colder fluid tends to stagnate in the lower right-hand section of the cavity between the baffle and the cold wall, resulting in a thermally stratified region and inhibiting the penetration of the warmer fluid from the cavity left-hand section. As a

consequence, a jet flow directed from the cold wall to the baffle tip is observed at Ra = 10^6. Even though the flow in the lower right-hand portion of the domain is weak, the stratification effects are not strong enough to cause separation. Note that the results obtained in this study presented in Figs. 4 and 5 are similar to results presented in Moukalled and Darwish (2003). From Tabs. 1 through 4, it can be seen that the average Nusselt numbers for both, buoyancy-assisting and opposing modes are also in good agreement with the ones obtained by Moukalled and Darwish (2003).

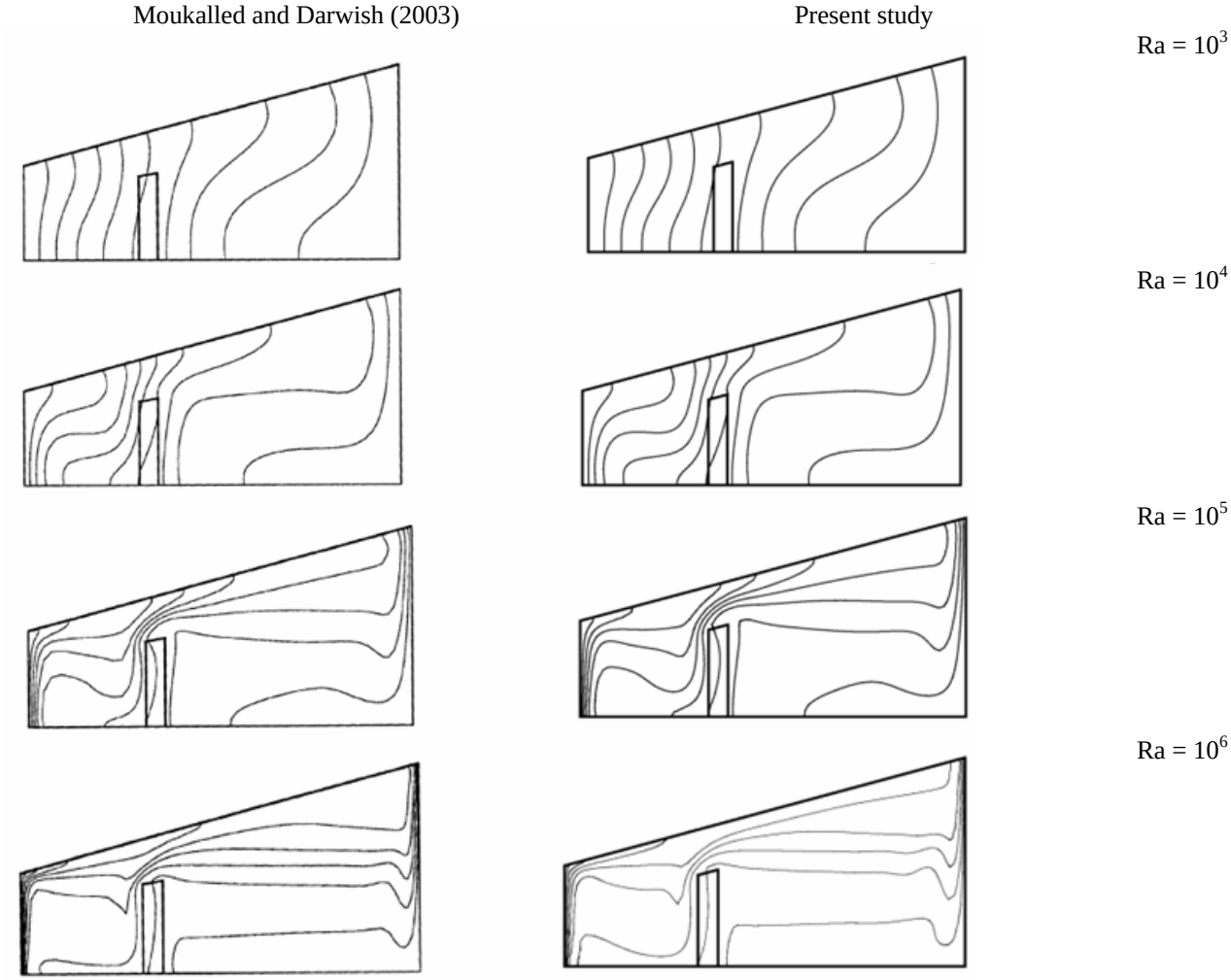

Figure 4. Isotherms (H_b = 2H*/3, L_b = L/3) for the buoyancy-assisting boundary condition.

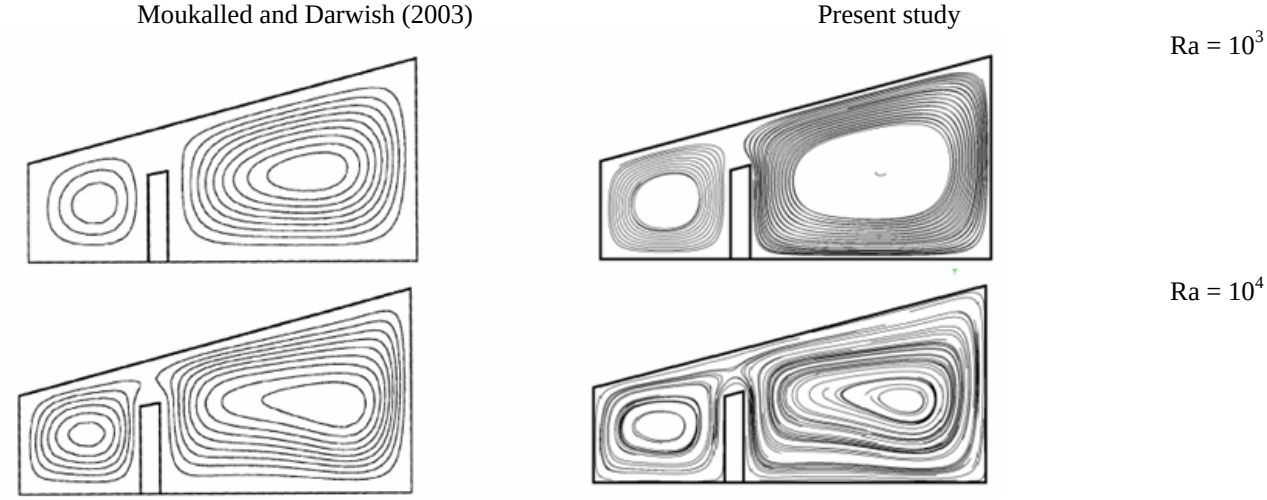

Figure 5. Streamlines (H_b = 2H*/3, L_b = L/3) for the buoyancy-assisting boundary condition.

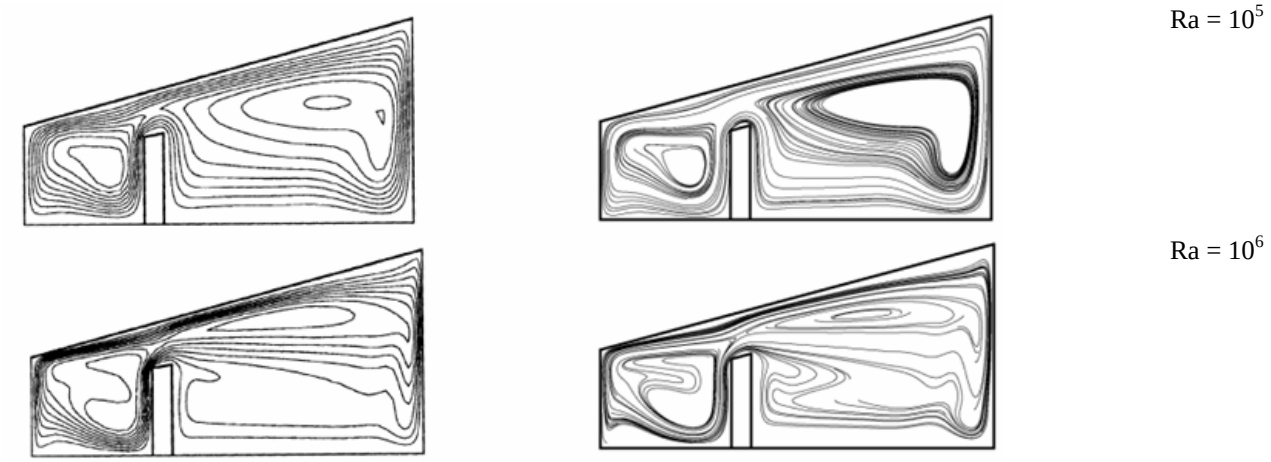

Figure 5. (cont.) Streamlines (H_b = 2H*/3, L_b = L/3) for the buoyancy-assisting boundary condition.

Table 1. Average Nusselt number values ($\overline{Nu}$) for cold left (short) wall and hot right (tall) wall (buoyancy-opposing boundary condition) for Pr = 0.7 and L_b = L/3.

	Moukalled and Darwish (2003)			Present study		
Ra	H_b = H*/3	H_b = 2H*/3	H_b = 0	H_b = H*/3	H_b = 2H*/3	H_b = 0
10^3	0.5080	0.4790	0.6153	0.5030	0.4829	0.6175
10^4	1.4750	0.9880	1.9220	1.4517	1.0140	1.9223
10^5	3.6780	2.1456	4.4310	3.4042	2.3144	4.3409

Table 2. Average Nusselt number values ($\overline{Nu}$) for cold left (short) wall and hot right (tall) wall (buoyancy-opposing boundary condition) for Pr = 0.7 and L_b = 2L/3.

	Moukalled and Darwish (2003)			Present study		
Ra	H_b = H*/3	H_b = 2H*/3	H_b = 0	H_b = H*/3	H_b = 2H*/3	H_b = 0
10^3	0.5040	0.4640	0.6153	0.5037	0.4710	0.6175
10^4	1.5510	1.0720	1.9220	1.5619	1.1080	1.9223
10^5	3.5640	2.2940	4.4310	3.6236	2.4361	4.3409

Table 3. Average Nusselt number values ($\overline{Nu}$) for cold right (tall) wall and hot left (short) wall (buoyancy-assisting boundary condition) for Pr = 0.7 and L_b = 2L/3.

	Moukalled and Darwish (2003)			Present study		
Ra	H_b = H*/3	H_b = 2H*/3	H_b = *0*	H_b = H*/3	H_b = 2H*/3	H_b = *0*
10^3	0.5670	0.4900	0.7150	0.5676	0.4976	0.7167
10^4	2.2560	1.3050	2.4800	2.2801	1.3127	2.5068
10^5	5.1660	3.9450	5.4760	5.3670	4.0084	5.6942

Table 4. Average Nusselt number values ($\overline{Nu}$) for cold right (tall) wall and hot left (short) wall (buoyancy-assisting boundary condition) for Pr = 0.7 and L_b = L/3.

	Moukalled and Darwish (2003)			Present study		
Ra	H_b = H*/3	H_b = 2H*/3	H_b = *0*	H_b = H*/3	H_b = 2H*/3	H_b = *0*
10^3	0.5460	0.5030	0.7150	0.5368	0.5033	0.7167
10^4	2.1420	1.1310	2.4800	2.1324	1.1542	2.5068
10^5	5.3030	3.5570	5.4760	5.4902	3.8112	5.6942

3.3. Comparing isotherms and streamlines for two baffles

Figures 6 and 7 present the isotherms and streamlines, respectively, and Fig. 8 shows the local Nusselt number for Rayleigh numbers changing from 10^3 through 10^6, for buoyancy-assisting and opposing modes. As physically expected the second baffle enhance the fluid flow and therefore increase the local Nusselt number when compared with the situation with only one baffle. The presence of secondary vortices, for buoyancy-assisting and opposing are also observed when the Rayleigh number is increased. A presence of much more stratified thermal field is also verified.

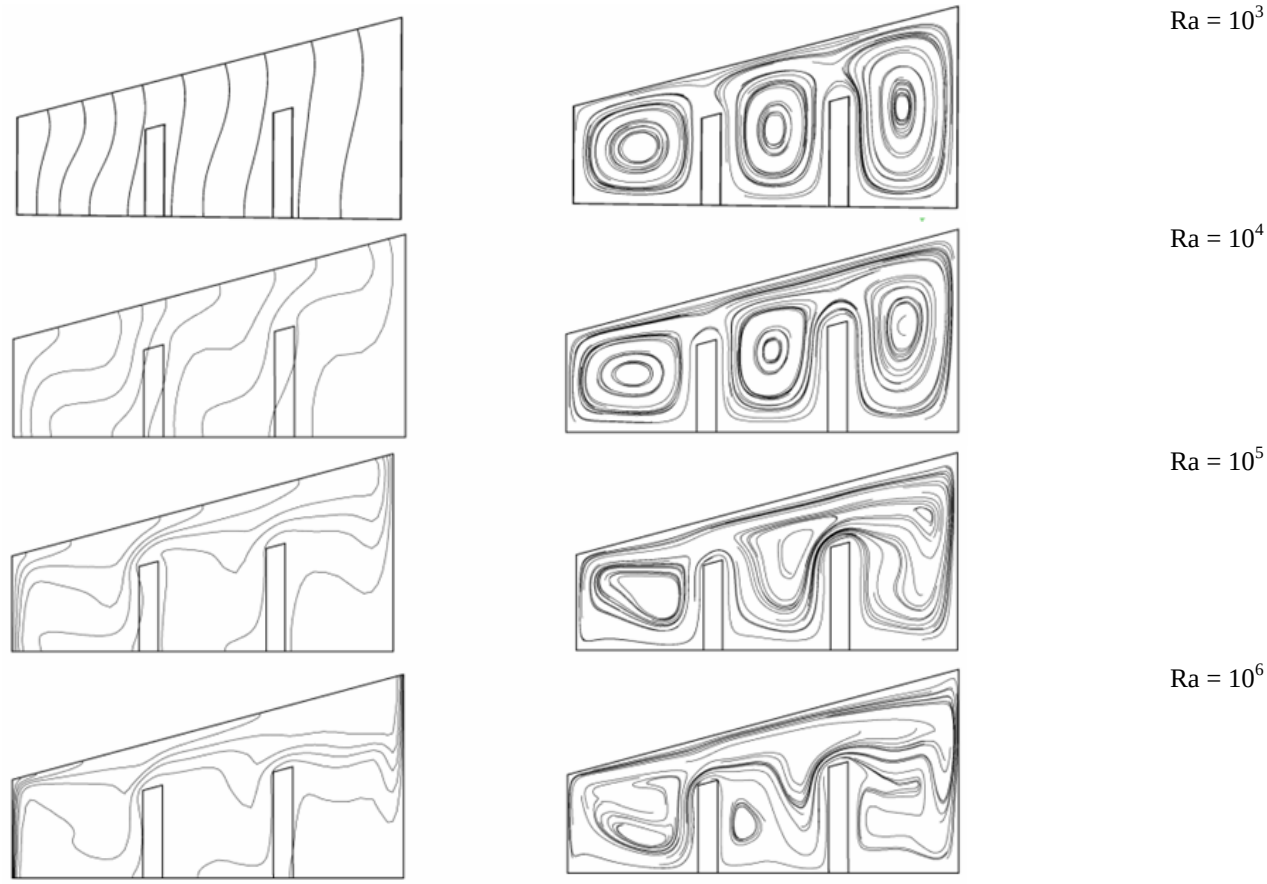

Figure 6. Isotherms and streamlines ($H_{b1} = H_{b2} = 2H^*/3$, $L_{b1} = L/3$ and $L_{b2} = 2L/3$) for the buoyancy-assisting boundary condition (left hot).

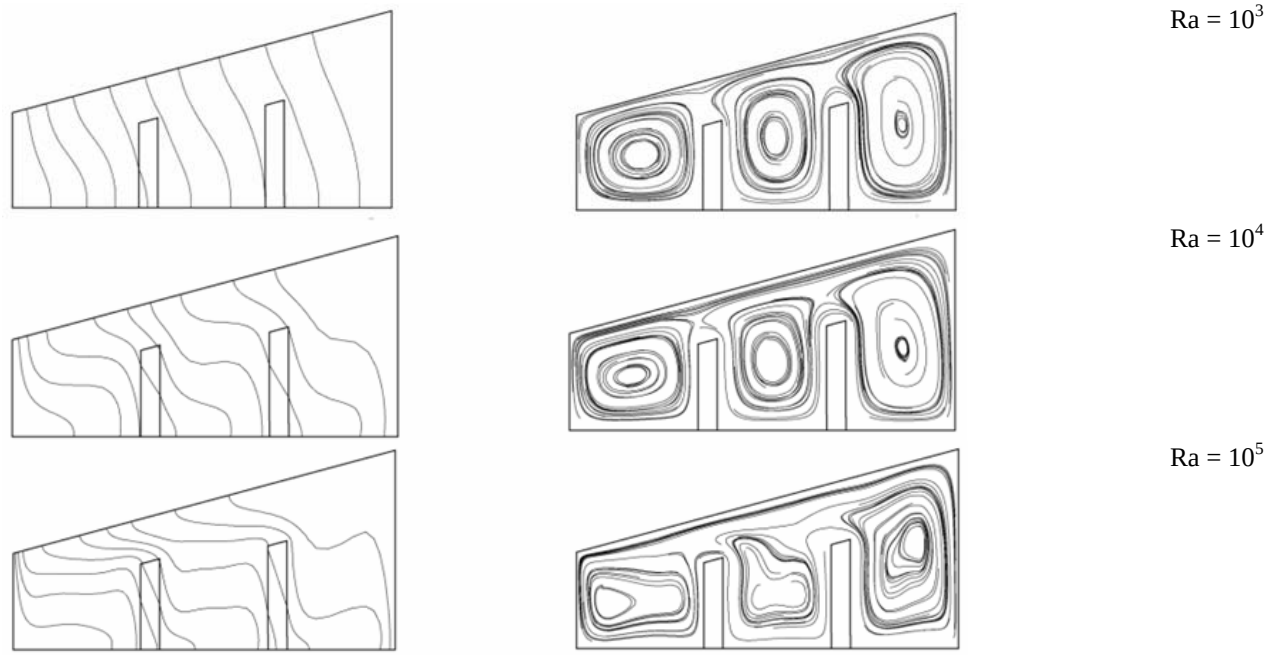

Figure 7. Isotherms and streamlines ($H_{b1} = H_{b2} = 2H^*/3$, $L_{b1} = L/3$ and $L_{b2} = 2L/3$) for the buoyancy-opposing boundary condition (right hot).

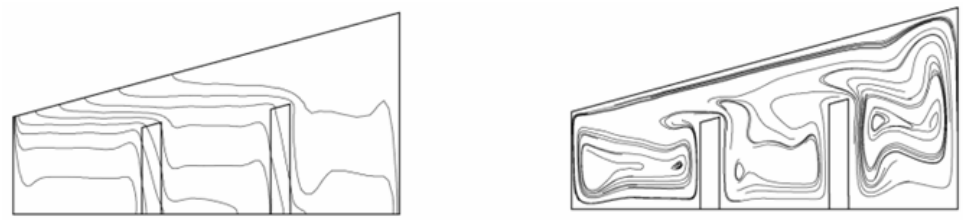

Figure 7. (cont.) Isotherms and streamlines ($H_{b1} = H_{b2} = 2H^*/3$, $L_{b1} = L/3$ and $L_{b2} = 2L/3$) for the buoyancy-opposing boundary condition (right hot).

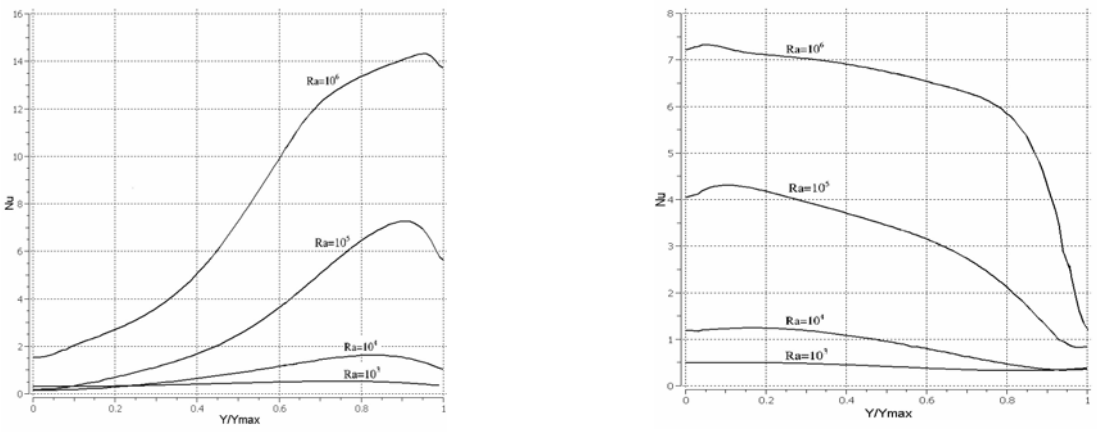

(a) (b)

Figure 8. Local Nusselt number along the (a) cold wall and (b) hot wall for the buoyancy-assisting boundary condition (left hot).

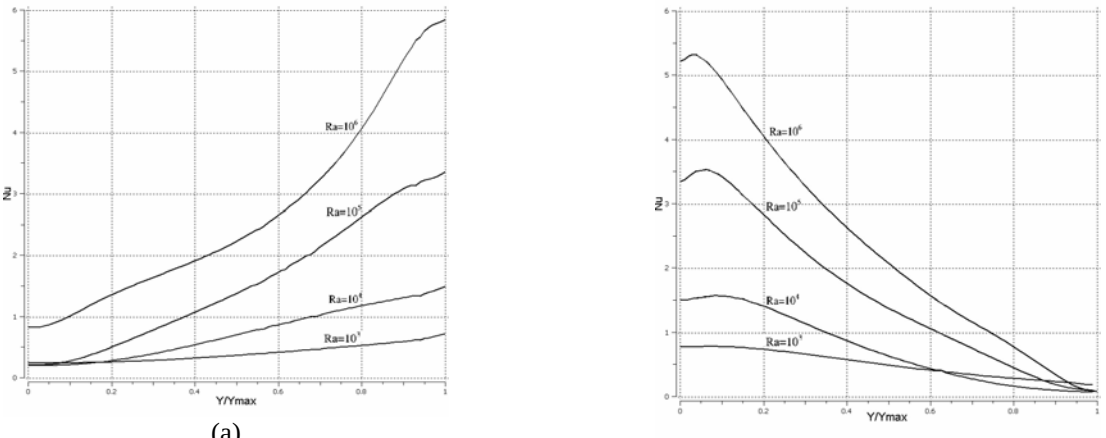

(a) (b)

Figure 9. Local Nusselt number along the (a) cold wall and (b) hot wall for the buoyancy-opposing boundary condition (right hot).

4. CONCLUSIONS

The natural convection in partitioned trapezoidal cavities with one and two internal baffles has been investigated in the present work. The conservation equations in terms of the primitive variables were solved by the finite-volume method. Several physical parameters, such as the number of baffles, boundary conditions (buoyancy-assisting opposing modes), position of the baffles were investigated. The results were presented in terms of isotherms, streamlines, and local and average Nusselt number. From the results, it was to observe that the second baffle intensify the fluid flow and the heat transfer inside the cavity. Also, the thermal stratification phenomenon is much more pronounced when compared with the situation with just only one baffle.

5. REFERENCES

Bejan, A., 2004, “Convection Heat Transfer”, 3rd ed., Wiley, Hoboken, NJU.

Boussaid, M., Djerrada, A. and Bouhadef, M., 2003, "Thermosolutal transfer within trapezoidal cavity", Numer. Heat Transfer A, Vol. 43, pp. 431–448.

Cormack, D.E., Leal, L.G. and Imberger, J., 1974, "Natural convection in a shallow cavity with differentially heated end walls". Part 1. Asymptotic theory, J. Fluid Mech., Vol. 65, pp. 209–229.

Del Campo, E.M., Sen, M. and Ramos, E., 1988, "Analysis of laminar natural convection in a triangular enclosure", Numer. Heat Transfer, Vol. 13, pp. 353–372.

Fusegi, T., Hyun, J.M. and Kuwahara, K., 1992, "Natural convection in a differentially heated square cavity with internal heat generation", Numer. Heat Transfer A, Vol. 21, pp. 215–229.

Gebhart, B., 1979, "Buoyancy induced fluid motions characteristics of applications in technology": the 1978 Freeman Scholar Lecture, ASME J. Fluids Eng., Vol., 101, pp. 5–28.

Hall, J.D., Bejan, A. and Chaddock, J.B., 1988, "Transient natural convection in a rectangular enclosure with one heated side wall", Int. J. Heat Fluid Flow, Vol. 9, pp. 396–404.

Hoogendoorn, C.J., 1986, "Natural convection in enclosures", Proceedings of Eighth International Heat Transfer Conference, vol. I, Hemisphere Publishing Corporation, San Francisco, pp. 111–120.

Holtzman, G.A., Hill, R.W. and Ball, K.S., 2000, "Laminar natural convection in isosceles triangular enclosures heated from below and symmetrically cooled from above", J. Heat Transfer, Vol. 122, pp. 485–491.

Hyun, J.M. and Lee, J.W., 1989, "Numerical solutions of transient natural convection in a square cavity with different sidewall temperature", Int. J. Heat Fluid Flow, Vol. 10, pp. 146–151.

Iyican, L., Bayazitoglu, Y. and Witte, L.C., 1980, "An analytical study of natural convective heat transfer within trapezoidal enclosure", J. Heat Transfer, Vol. 102, pp. 640–647.

Iyican, L., Witte, L.C. and Bayazitoglu, Y., 1980, "An experimental study of natural convection in trapezoidal enclosures", J. Heat Transfer, Vol. 102, pp. 648–653.

Karyakin, Yu.E., Sokovishin, Yu.A. and Martynenko, O.G., 1988, "Transient natural convection in triangular enclosures", Int. J. Heat Mass Transfer, Vol. 31, pp. 1759–1766.

Karyakin, Yu.E., 1989, "Transient natural convection in prismatic enclosures of arbitrary cross-section", Int. J. Heat Mass Transfer, Vol. 32, pp. 1095–1103.

Kuyper, R.A. and Hoogendoorn, C.J., 1995, "Laminar natural convection flow in trapezoidal enclosures", Numer. Heat Transfer A, Vol. 28, pp. 55–67.

Lage, J.L. and Bejan, A., 1991, "The Ra–Pr domain of laminar natural convection in an enclosure heated from the side", Numer. Heat Transfer A, Vol. 19, pp. 21–41.

Lam, S. W., Gani, R. and Simons, J. G., 1989, "Experimental and numerical studies of natural convection in trapezoidal cavities", J. Heat Transfer, Vol. 111, pp. 372–377.

Lee, T. S., 1991, "Numerical Experiments with Fluid Convection in Tilted Nonrectangular Enclosures", Numer. Heat Transfer A, Vol. 19, pp. 487–499.

Lee, T.S., 1984, "Computational and Experimental Studies of Convective Fluid Motion and Heat Transfer in Inclined Non-Rectangular Enclosures", Int. J. Heat Fluid Flow, Vol. 5, pp. 29–36.

Moukalled, F. and Acharya, S., 1997, "Buoyancy-induced heat transfer in partially divided trapezoidal cavities", Numer. Heat Transfer A, Vol. 32, pp. 787–810.

Moukalled, F. and Acharya, S., 2000, "Natural convection in trapezoidal cavities with baffles mounted on the upper inclined surfaces", Numer. Heat Transfer A, Vol. 37, No. 6, pp. 545–565.

Moukalled, F. and Acharya, S., 2001, "Natural convection in a trapezoidal enclosure with offset baffle", AIAA J. Thermophys. Heat Transfer, Vol. 15, No. 2, pp. 212–218.

Nicolette, V.F, Yang, K.T. and Lloyd, J.R., 1985, "Transient cooling by natural convection in a two-dimensional square enclosure", Int. J. Heat Mass Transfer, Vol. 28, pp. 1721–1732.

Ostrach, S., 1988, "Natural convection in enclosures", J. Heat Transfer, Vol. 110, pp. 1175–1190.

Patterson, J. and Imberger, J., 1980, "Unsteady natural convection in a rectangular cavity", J. Fluid Mech., Vol. 100, pp. 65–86.

Peric, M., 1993, "Natural convection in trapezoidal cavities", Numer. Heat Transfer A, Vol. 24, pp. 213–219.

Poulikakos, D. and Bejan, A., 1983, "The fluid dynamics of an attic space", J. Fluid Mech., Vol. 131, pp. 251–269.

Xia, C. and Murthy, J.Y., 2002, "Buoyancy-driven flow transitions in deep cavities heated from below", ASME J. Heat Transfer, Vol. 124, pp. 650–659.

6. RESPONSIBILITY NOTICE

The authors, Éliton Fontana, Adriano da Silva, Andre de Souza Araújo, Francisco Marcondes, and Viviana Cocco Mariani are the only responsible for the printed material included in this paper.